Available online at www.sciencedirect.com
ScienceDirect
Ceramics International 37 (2011) 3229–3235
CERAMICS INTERNATIONAL
www.elsevier.com/locate/ceramint

Pressureless sintering of B_4C–TiB_2 composites with Al additions

Mehri Mashhadi [a,*], Ehsan Taheri-Nassaj [a], Maryam Mashhadi [b], Vincenzo M. Sglavo [c]

[a] Department of Materials Engineering, Faculty of Engineering, Tarbiat Modares University, Tehran, Iran
[b] Department of Applied Chemistry, Faculty of Science, Center Tehran Branch, Islamic Azad University, Tehran, Iran
[c] Department of Materials Engineering and Industrial Technologies, University of Trento, Trento, Italy

Received 24 May 2010; received in revised form 14 March 2011; accepted 24 March 2011
Available online 27 May 2011

Abstract

The effects of Al addition on pressureless-sintering of B_4C–TiB_2 composites were studied. Different amounts of Al from 0% to 5 wt.% were added to B_4C–TiB_2 mixtures (containing up to 30 wt.% TiB_2) and the samples were pressureless sintered at 2050 °C and 2150 °C under Ar atmosphere. Physical, microstructural and mechanical properties were analysed and correlated with TiB_2 and Al additions and sintering temperature. Addition of Al to B_4C–TiB_2 results in increased shrinkage upon sintering and final relative density and lower porosity, the effect is being more evident when both Al and TiB_2 are present. Fracture strength, elastic modulus and fracture toughness of 450 MPa, 500 GPa and 6.2 MPa.$m^{1/2}$, respectively were measured.

Keywords: C. Mechanical properties; B_4C; TiB_2; Ceramic composites; Pressureless sintering

1. Introduction

Boron carbide is an important non-metallic hard material with high melting point and hardness and low density as well as high chemical resistance [1]. Due to the outstanding properties, B_4C ceramics are good candidate for many structural applications. Boron carbide can be used as neutron absorber, armor, abrasive media for lapping and grinding, polishing media for hard materials and wear resistant components [2–5]. However, this wide range of applications is restricted by limited strength and fracture toughness as well as by poor sinterability and machinability [6]. In order to promote densification at relatively low temperatures, different sintering additives have been proposed such as Si, Al, Mg, Ni, Al_2O_3, SiC, SiC + Al, TiB_2, TiB_2 + C, ZrB_2, W_2B_5, B, BN [5–16]. Among the studied systems, B_4C–TiB_2 composites attracted the attention of materials scientists because of the very interesting mechanical properties associated to micro-cracking behaviour that accounts for appealing for high fracture toughness values [17–20].

Boron carbide–aluminium cermets have the potential for offering a combination of high hardness and toughness in a lightweight structure. Aluminium has been incorporated into B_4C matrix ceramics as a second phase for pressureless sintering [21–25] or to improve the performances of B_4C matrix ceramics by hot pressing [26].

In the present paper, the influence of Al addition on the densification behaviour, physical and mechanical properties of pressureless sintered B_4C–TiB_2 composites is investigated. Both Al and TiB_2 additions to B_4C matrix provides high flexural strength, high fracture toughness and fine and dense microstructure, simultaneously.

2. Experimental procedures

High-purity B_4C (Chengdu Greenworld Chemical, China, B:C = 3.8–3.9, average particle size = 1.3 μm), and TiB_2 (Chengdu Greenworld Chemical, China, 98% pure and particle size < 3 μm) powders were used as starting materials. Al powder (99.5% and particle size < 1 μm) was used as sintering aid. Composites were prepared using different amounts (from 5 to 30 wt.%) of TiB_2 and Al (from 1 to 5 wt.%). The powders were mixed with high-purity phenolic resin binder and methanol in a WC planetary mill for 1 h [22,23] and then uniaxially cold pressed under 80 MPa to prepare

* Corresponding author.
E-mail address: me_mashadi@yahoo.com (M. Mashhadi).

0272-8842/$36.00
doi:10.1016/j.ceramint.2011.05.096

Table 1
Crystalline phases detected by XRD analysis in sintered B_4C–TiB_2 composites.

Sample no.	B_4C (wt.%)	TiB_2 (wt.%)	Al (wt.%)	Sintering temperature (°C)	Phases
1	69	30	1	2050	B_4C, TiB_2, graphite
2	90	5	5	2050	B_4C, TiB_2, graphite, $Al_8B_4C_7$
3	65	30	5	2050	B_4C, TiB_2, graphite, $Al_8B_4C_7$
4	65	30	5	2150	B_4C, TiB_2, graphite, $Al_8B_4C_7$

The present phases in B_4C–TiB_2 composites sintered at different temperatures and containing different values of TiB_2 and Al.

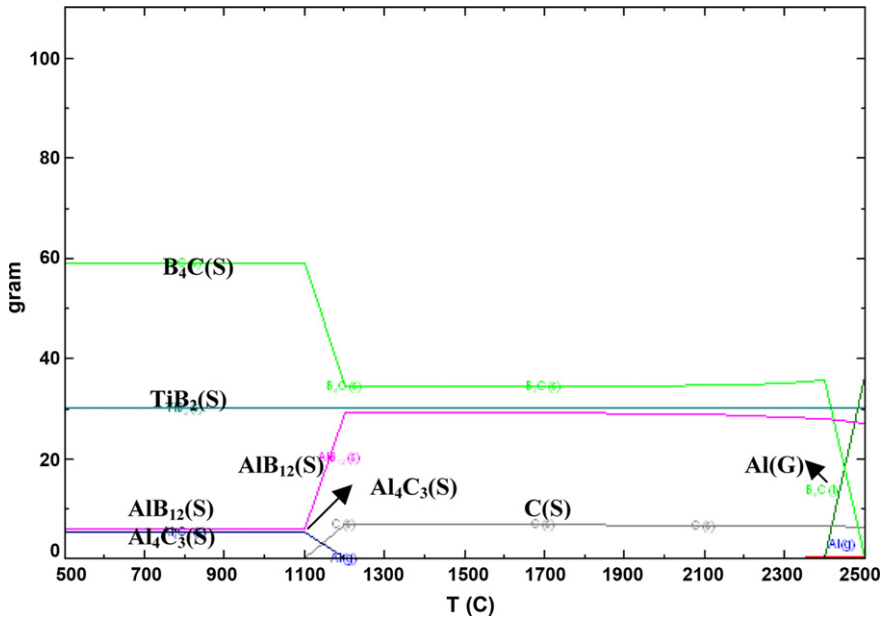

Fig. 1. The present phases in B_4C–TiB_2–Al system as a function of temperature obtained by FactSage software.

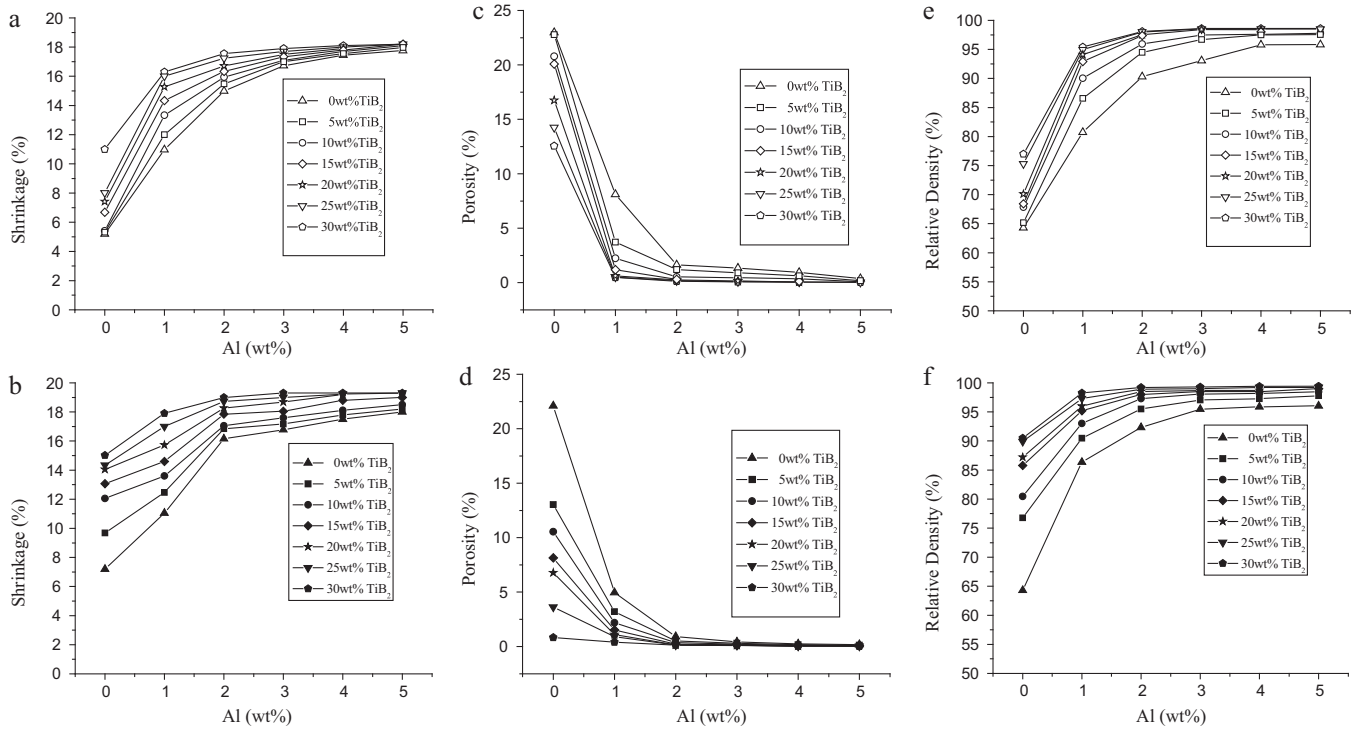

Fig. 2. Effect of Al and TiB_2 on: (a and b) shrinkage; (c and d) porosity; (e and f) relative bulk density. (Open and solid symbols are related to 2050 °C and 2150 °C sintering temperature, respectively.)

50 mm × 50 mm × 10 mm samples. The plates were then CIPed at 180 MPa. Each plate was cut into bars of 10 mm × 10 mm × 50 mm which were then polished by SiC paper (320 grits) to remove macroscopic surface defects. Samples were then heated for 1 h at 900–1000 °C to burn out the phenolic resin binder and sintered in a graphite elements furnace under Ar atmosphere at 2050 and 2150 °C for 1 h (heating rate = 10 °C/min).

Sintered bodies were surface ground and polished with diamond paste down to 1 μm grain size for successive

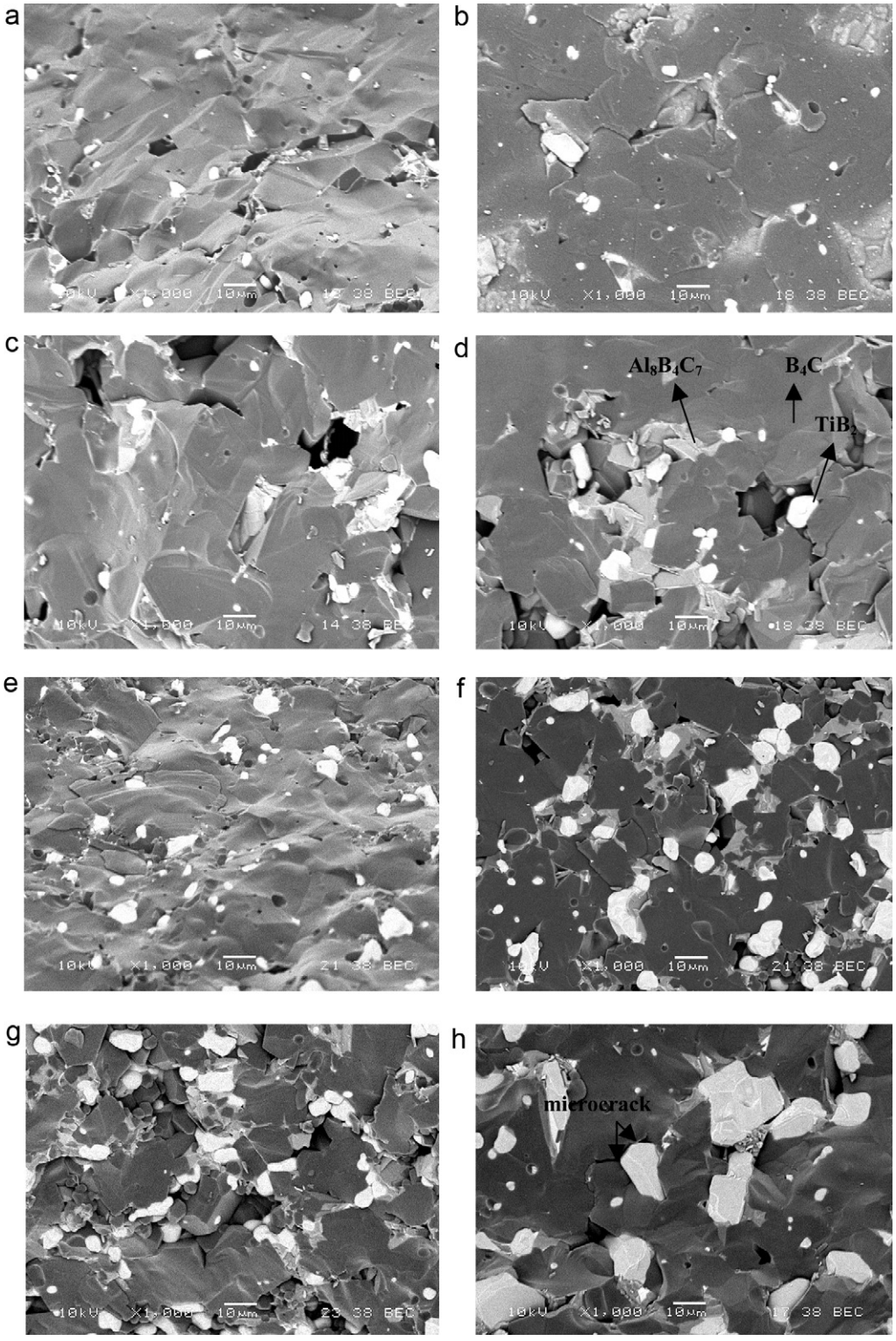

Fig. 3. SEM micrographs of composites (sintering temperature = 2050 °C) fracture surfaces containing TiB_2 and Al loads equal to: (a) 10 and 2 wt.%; (b)10 and 3 wt.%; (c) 10 and 4 wt.%; (d) 10 and 5 wt.%; (e) 20 and 4 wt.%; (f) 25 and 4 wt.%; (g) 30 and 4 wt.% and (h) 30 and 4 wt.% (2150 °C).

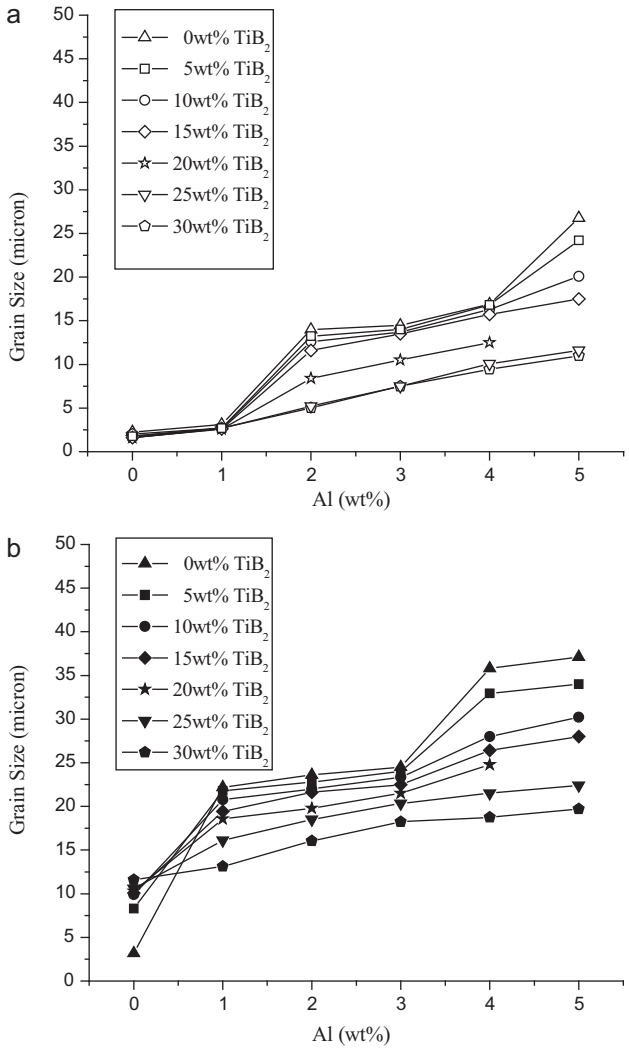

Fig. 4. Effect of Al additions on grain size of sintered composites at: (a) 2050 °C and (b) 2150 °C.

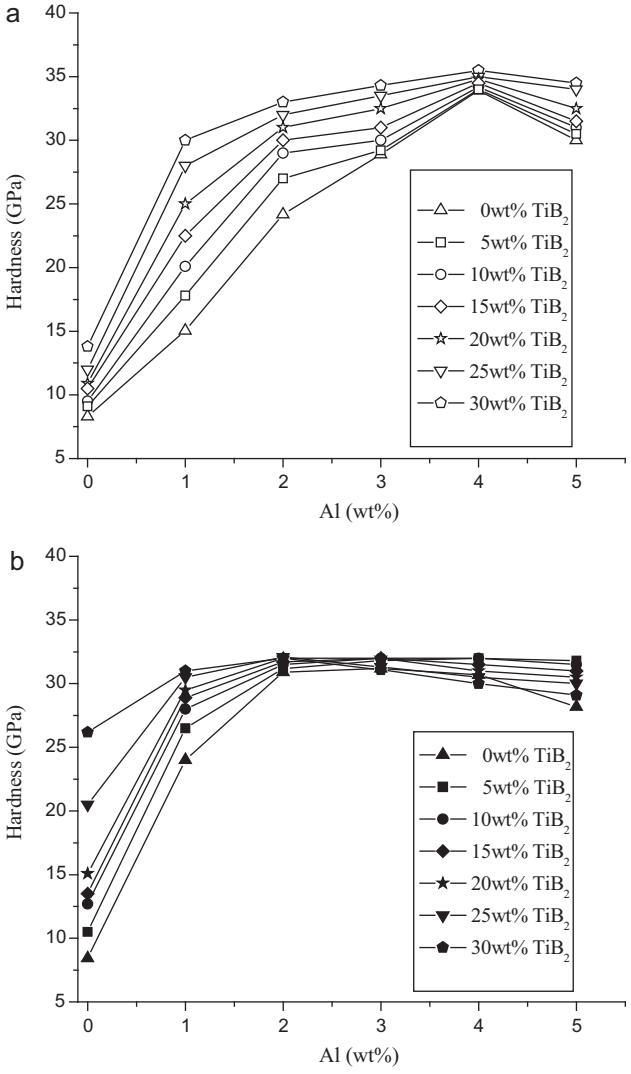

Fig. 5. Effect of Al additions on hardness of B_4C–TiB_2 composites sintered at: (a) 2050 °C and (b) 2150 °C.

microstructure examinations. The polished surfaces were then electrochemically etched in a 0.1% KOH water solution with current density of 0.1 A/cm^2 for 60–120 s.

The microstructure was observed under scanning electron microscope (SEM) (JEOL, JSM-5500) and chemical composition was qualitatively determined by energy dispersive X-ray spectroscopy (EDXS). Mean grain size of sintered samples was calculated by using the line intercept method on SEM micrographs [27].

Bulk and apparent density and open porosity of the samples were measured by Archimede's method.

Crystalline phases were characterized by X-ray diffraction (XRD) (Philips, model Xpert).

Bars with sizes of 3 mm × 4 mm × 45 mm were cut from sintered samples and polished with diamond paste down to 1 μm grain size. Care was also used to uniformly chamfer the edges at about 45°. Vickers indentation (maximum load = 30–100 N) was used to measure hardness and fracture toughness [28]. Indentation imprint and crack length were determined from an average of 10 test for each composition.

Strength and elastic modulus were measured by four-point bending test by using a universal testing machine (MTS System, Model 810) with a crosshead speed of 1 mm/min. Inner and outer spans were 20 and 40 mm, respectively. At least five samples for each composition were considered.

3. Results and discussion

Table 1 shows the crystalline phases detected by XRD in the B_4C–TiB_2 composites and one can easily observe the presence of graphite probably deriving either from decomposition of the residual phenolic resin or from B_4C and $Al_8B_4C_7$ phases as the result of possible reactions between Al and B_4C [29–31]. In order to analyse such a result, the phases were analysed by using the FactSage thermochemical software [32] which provides determining the most favourable phases (in terms of free energy) as a function of temperature, initial composition and environment. The present phases at sintering temperature are shown in Fig. 1. One can observe that at relatively low

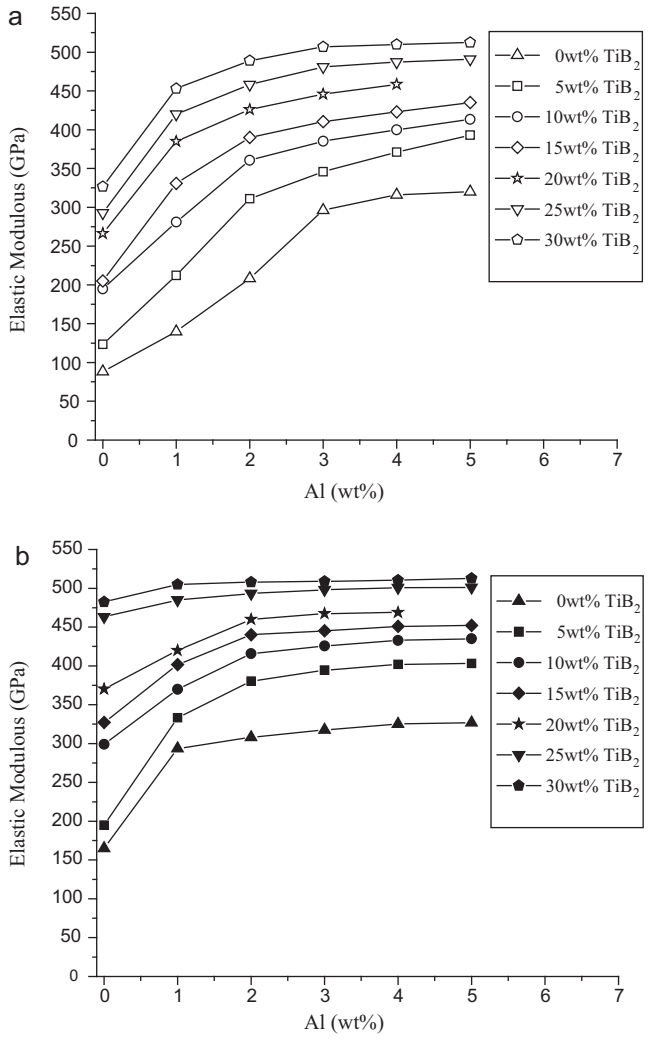

Fig. 6. Effect of Al additions on elastic modulus of B_4C–TiB_2 composites sintered at: (a) 2050 °C and (b) 2150 °C.

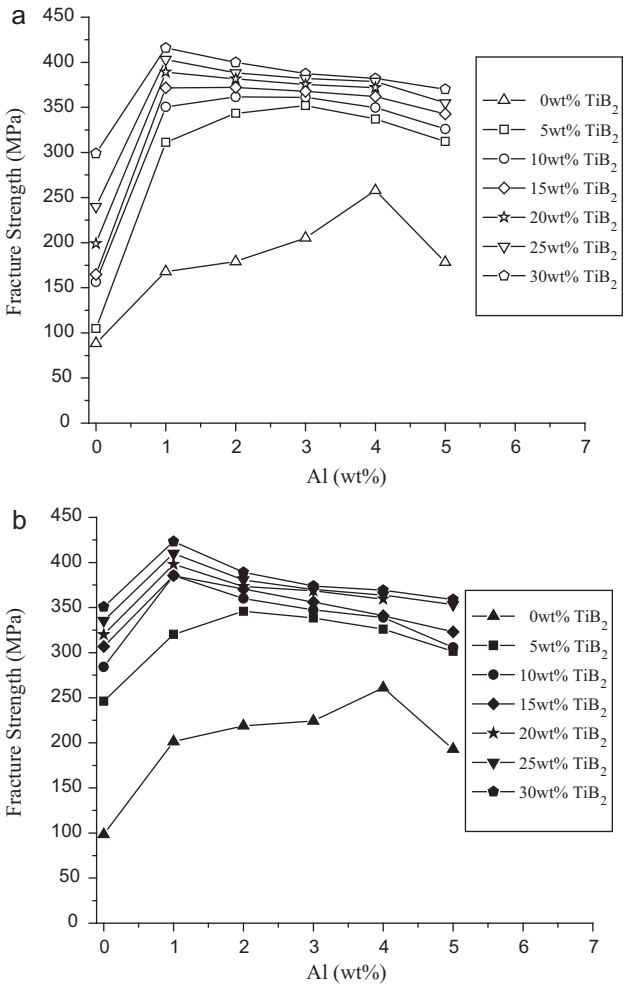

Fig. 7. Effect of Al additions on fracture strength of B_4C–TiB_2 composites; sintering temperature = (a) 2050 °C and (b) 2150 °C.

temperatures B_4C reacts with Al according to:

$$3B_4C + 5Al \rightarrow Al_4C_3 + AlB_{12} \quad (1)$$

B_4C, Al_4C_3 and AlB_{12} phases are inert up to 1100 °C when B_4C reacts with Al_4C_3 to yield AlB_{12} and carbon:

$$12B_4C + Al_4C_3 \rightarrow 4AlB_{12} + 15C \quad (2)$$

TiB_2 is thermodynamically stable during the heat treatment and does not undergo any change. After sintering and during cooling the samples to room temperature, AlB_{12} can react with carbon to produce B_4C and $Al_8B_4C_7$:

$$8AlB_{12} + 30C \rightarrow Al_8B_4C_7 + 23B_4C \quad (3)$$

This can be the main reason for observing $Al_8B_4C_7$ phase in XRD results. Because the phase analysis has been conducted at room temperature and only stable phases at room temperature can be presented and detected by this method.

The effect of Al additions on shrinkage upon sintering, porosity and bulk density are shown in Fig. 2. As expected shrinkage upon sintering increases for sintering temperature rising from 2050 to 2150 °C. Al additions have a profound effect on shrinkage upon sintering, the effect being more limited when large quantities of TiB_2 are present. In other words both Al and TiB_2 promote sintering of B_4C matrix, the maximum shrinkage is being recorded when 5 wt.% Al is used to B_4C-30 wt.%TiB_2 composite.

The effects are clear also regarding to open porosity and bulk density (Fig. 2c–d). One can observe that Al addition an excess of 2 wt.% allows the production of almost fully dense composite, especially for the largest amounts of TiB_2 reinforcing phase and at 2150 °C sintering temperature.

The microstructure of B_4C–TiB_2 composites is shown in Fig. 3. One can confirm that the addition of Al leads to decrease the porosity of the sintered material. By adding 5 wt.% Al, porosity decreases to about zero.

Fig. 4 shows the effect of Al addition on the average grain size. The grain size of B_4C–TiB_2 composites sintered at 2050 °C is about 2 μm and does not sensibly change with Al load lower than 1% at the same sintering temperature. Conversely, additions of Al between 2% and 4% lead to larger

grain size especially for limited amount of reinforcing phase (TiB_2) that, therefore, acts as grain growth inhibitor. At higher sintering temperature (2150 °C) the effect is similar though grain growth is evidently beginning from 1% Al addition due to the activation of diffusion processes.

Fig. 5 shows the effect of Al additions on hardness. As expected, the addition of Al has a positive effect on Vickers hardness that consists of almost 5 wt.% Al loads. This effect can be accounted for the density increase previously pointed out. Quite surprisingly hardness increases also with TiB_2 content, especially for composites sintered at 2050 °C, though the reinforcing phase hardness is lower than B_4C matrix one. Nevertheless, also such behaviour can be related to the denser microstructure obtained by TiB_2 addition.

Similarly to density and hardness, Al addition has a positive effect also on elastic modulus (Fig. 6) and similar explanations can be reported in the present case [33].

The effect of Al additions on fracture strength is shown in Fig. 7. An intensive increase occurs for limited additions of Al (1 wt.%) while strength remains substantially constant for further Al loads. One can also observe that strength is always higher when larger amount of reinforcing phase (TiB_2) is present. An important effect responsible for increasing failure stress is related to the decrease the porosity and, therefore, of flaws within the material associated with beneficial sintering promoted by Al addition. In addition, strength data can be correlated with fracture toughness results (Fig. 8). Al addition has important effects also on fracture toughness, this is being associated with elastic modulus/density increase. Nevertheless, one should point out the important effect of the reinforcing phase that allows to duplicate fracture toughness when TiB_2 additions as high as 30 wt.% are used. Both fracture energy (G_C) and elastic modulus (E) contribute to fracture toughness through the well-known relationship:

$$K_C = \sqrt{GE} \tag{4}$$

One can observe that if the elastic modulus doubles, K_C should be increased by a factor of ≈1.4. If data in Figs. 6 and 8 are compared, it is possible to conclude that, though limited, there is an additional contribution to fracture toughness other than the elastic modulus increase as a function of TiB_2 content. Such contribution can be associated with toughening effect typically observed in B_4C–TiB_2 composites such as micro-cracking [34] which is probably limited in the materials considered here due to the presence of porosity and spurious phases like $Al_8B_4C_7$ previously were pointed out.

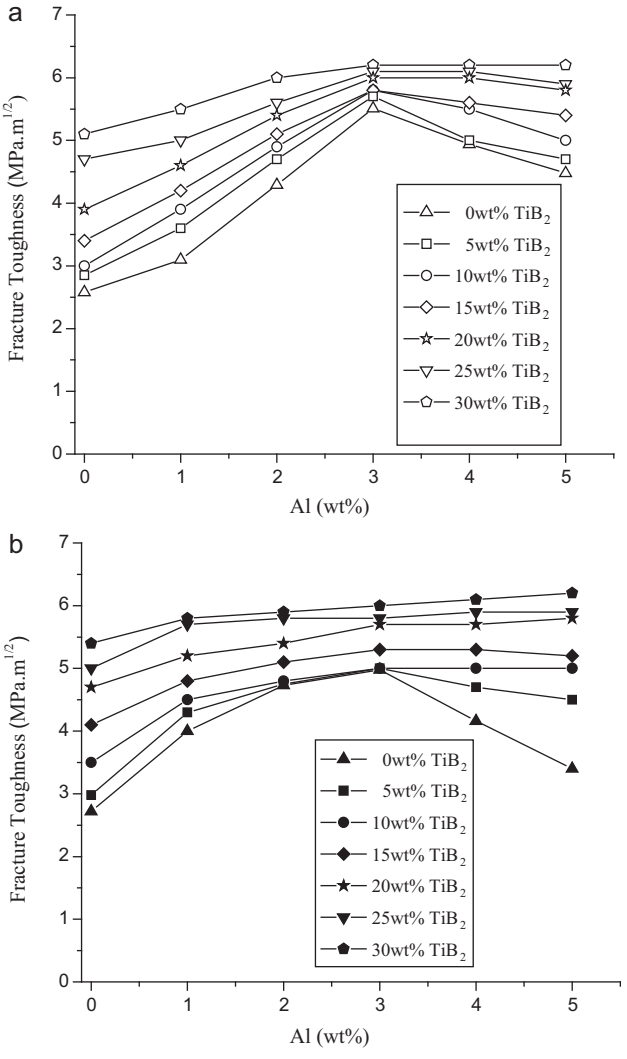

Fig. 8. Effect of Al additions on fracture toughness of B_4C–TiB_2 composites sintered at: (a) 2050 °C and (b) 2150 °C.

4. Conclusion

- In B_4C–TiB_2–Al system, Al reacts with B_4C and $Al_8B_4C_7$ and carbon phases are formed, but there is not any reaction between TiB_2 and B_4C.
- Adding Al to B_4C–TiB_2 composites results in increasing the shrinkage and the relative density and decreasing the porosity.
- Increasing TiB_2 phase leads in less grain growth.
- In samples containing different amounts of TiB_2, Al addition of at least 1 wt.% increases the fracture strength considerably.
- The fracture mode in B_4C–TiB_2 samples containing Al is transgranular and intergranular.
- In the presence of Al and TiB_2 phases in B_4C matrix, maximum values of fracture strength, elastic modulus, hardness and fracture toughness were obtained of about 450 MPa, 500 GPa, 35 GPa and 6.2 MPa.m$^{1/2}$ respectively.
- In pressureless sintering of B_4C–TiB_2 composites, grain growth can be controlled by TiB_2 phase and Al improves the sintering behaviour.

References

[1] F. Thevenot, Boron carbide—a comprehensive review, J. Eur. Ceram. Soc. 6 (1990) 205–225.
[2] A.J. Pyzik, I.A. Aksay, Multipurpose Boron Carbide–Aluminium Composite and its Manufacture via the Control of the Microstructure, US Patent No. 4,702,770 (1987).
[3] D.C. Halverson, A.J. Pyzik, I.A. Aksay, W.E. Snowden, Processing of boron carbide–aluminium composites, J. Am. Ceram. Soc. 72 (5) (1989) 775–780.

[4] F. Thevenot, Sintering of boron carbide–silicon carbide two-phase materials and their properties, J. Nucl. Mater. 152 (1988) 154–162.
[5] Y. Kanno, K. Kawase, K. Nakano, Additive effect on sintering of boron carbide, Yogyo-Kyokai-Shi 95 (11) (1987) 1137–1140.
[6] S. Yamada, K. Hirao, Y. Yamauchi, S. Kanzaki, Mechanical and electrical properties of B_4C–CrB_2 ceramics fabricated by liquid phase sintering, Ceram. Int. 29 (2003) 299–304.
[7] T.K. Roy, C. Subramanian, A.K. Suri, Pressureless sintering of boron carbide, Ceram. Int. 32 (2006) 227–233.
[8] H. Suzuki, T. Hase, T. Maruyama, Effect of carbon on sintering of boron carbide, Yogyo-Kyokai-Shi 87 (8) (1979) 430–433.
[9] K.A. Schwetz, W. Grellner, The influence of carbon on the microstructure and mechanical properties of sintered boron carbide, J. Less-Common Met. 82 (1981) 37–47.
[10] B. Champagne, R. Angers, Mechanical properties of hot pressed B–B_4C materials, J. Am. Ceram. Soc. 62 (3-4) (1979) 149–153.
[11] L. Levin, N. Frage, M.P. Dariel, Novel approach for the preparation of B_4C-based cermets, Int. J. Refract. Met. Hard Mater. 18 (2000) 131–135.
[12] A. Goldstein, Y. Geffen, A. Goldenberg, Boron carbide–zirconium boride in situ composites by the reactive pressureless sintering of boron carbide zirconia mixtures, J. Am. Ceram. Soc. 84 (3) (2001) 642–644.
[13] Z. Zakhariev, D. Radev, Properties of polycrystalline boron carbide sintered in the presence of W_2B_5 without pressing, J. Mater. Sci. Lett. 7 (1988) 695–696.
[14] R. Ruh, M. Kearns, A. Zangvil, Y. Xu, Phase and property studies of boron carbide–boron nitride composites, J. Am. Ceram. Soc. 75 (4) (1992) 864–872.
[15] H.W. Kim, Y.H. Koh, H.E. Kim, Densification and mechanical properties of B_4C with Al_2O_3 as a sintering additives, J. Am. Ceram. Soc. 83 (11) (2000) 2363–2365.
[16] K. Lu, X. Zhu, K. Nagarathnam, Nickel–boron nanolayer-coated boron carbide pressureless sintering, J. Am. Ceram. Soc. 92 (7) (2009) 1500–1505.
[17] S. Tuffe, J. Dubois, G. Fantozzi, G. Barbier, Densification, microstructure and mechanical properties of TiB_2–B_4C based composites, Int. J. Refract. Met. Hard Mater. 14 (1996) 305–310.
[18] V. Skorokhod, V.D. Krstic, High strength-high toughness B_4C–TiB_2 composites, J. Mater. Sci. Lett. 19 (2000) 237–239.
[19] T.S. Srivatsan, G. Guruprasad, D. Black, R. Radhakrishnan, T.S. Sudarshan, Influence of TiB_2 content on microstructure and hardness of TiB_2–B_4C composite, Powder Technol. 159 (3) (2005) 161–167.
[20] H.R. Baharvandi, A.M. Hadian, Pressureless sintering of TiB_2–B_4C ceramic matrix composite, J. Mater. Eng. Perform. 17 (6) (2008) 838–841.
[21] D.C. Halverson, A.J. Pyzik, I.A. Aksay, Processing and microstructural characterization of B_4C–Al cermets, Ceram. Eng. Sci. Proc. 6 (1985) 736–744.
[22] M. Mashhadi, E. Taheri Nassaj, V.M. Sglavo, H. Sarpoolaky, N. Ehsani, Effect of Al addition on pressureless sintering of B_4C, Ceram. Int. 35 (2009) 831–837.
[23] M. Mashhadi, E. Taheri Nassaj, V.M. Sglavo, Pressureless sintering of boron carbide, Ceram. Int. 36 (2010) 151–159.
[24] B.S. Lee, S. Kang, Low temperature processing of B_4C–Al composites via infiltration technique, Mater. Chem. Phys. 67 (1–3) (2001) 249–255.
[25] J. Jung, S. Kang, Advances in manufacturing boron carbide–aluminum composites, J. Am. Ceram. Soc. 87 (1) (2004) 47–54.
[26] J. Sun, C. Liu, C. Duan, Effect of Al and TiO_2 on sinterability and mechanical properties of boron carbide, Mater. Sci. Eng. A 509 (2009) 89–93.
[27] J.C. Wurst, J.A. Nelson, Lineal intercept technique for measuring grain size in two-phase polycrystalline ceramics, J. Am. Ceram. Soc.-Discuss. Notes (1972) 109.
[28] H. Lee, R.F. Speyer, Hardness and fracture toughness of pressureless sintered boron carbide (B_4C), J. Am. Ceram. Soc. 85 (5) (2002) 1291–1293.
[29] H. Okamoto, Al–Ti (aluminium–titanium), J. Phase Equilib. 14 (1993) 120–121.
[30] V. Raghavan, Al–B–Ti (aluminium–boron–titanium), J. Phase Equilib. Diff. 26 (2) (2005) 173–174.
[31] I. Maxwell, A. Hellawell, The constitution of the system Al–Ti–B with reference to aluminium—base alloys, Metall. Trans. 3 (1972) 1487–1493.
[32] C.W. Bale, E. Belisle, P. Chartrand, S.A. Decterov, G. Eriksson, K. Hack, I.H. Jung, Y.B. Kang, J. Melancon, A.D. Pelton, C. Robelin, S. Petersen, FactSage thermochemical software and databases—recent developments, Calphad 32 (2) (2009) 295–311.
[33] S. Torquato, C.L.Y. Yeong, M.D. Rintoul, D.L. Milius, I.A. Aksay, Elastic properties and structure of interpenetrating boron carbide/aluminium multiphase composites, J. Am. Ceram. Soc. 82 (5) (1999) 1263–1268.
[34] L.S. Sigl, H.J. Kleebe, Microcracking in B_4C–TiB_2 composites, J. Am. Ceram. Soc. 78 (9) (1995) 2374–2380.